Fivefold differential cross section of fast $(e,2e)$ ionization of H_2, D_2, and T_2 by a Franck-Condon approach

P. Weck, B. Joulakian, and P. A. Hervieux
Institut de Physique, Laboratoire de Physique Moléculaire et des Collisions, Université de Metz, Technopôle 2000, 1 Rue Arago, 57078 Metz Cedex 3, France
(Received 6 April 1999)

The fivefold differential cross sections of the simple ionization of hydrogen, deuterium, and tritium diatomic molecules are determined by the use of one-center Coulomb continuum wave functions describing the slow ejected electron. Vertical transitions from the lowest vibrational state of the fundamental $^1\Sigma_g$ state of the target to the vibrational levels of the fundamental $^2\Sigma_g$ state of H_2^+, D_2^+, or T_2^+ are considered. The results obtained for two different energy resolutions (1 and 3 eV) show that the difference between these three species should increase with a decrease of the energy resolution. [S1050-2947(99)04410-8]

PACS number(s): 34.80.Dp

INTRODUCTION

Simple ionization of atoms by electron impact is one of the important processes of atomic physics. Besides its fundamental aspect, especially in the study of the electronic structure of the target, it is a powerful tool for the study of the mechanisms of ionization itself, whose comprehension becomes important in many domains such as plasma physics, fusion experiments, and even in the study of ionising collisions on living matter [1].

$(e,2e)$ experiments, which are simple ionization experiments with coincidence detection of the scattered and the ejected electron, have been performed for many atomic targets in the domain of the electron momentum spectroscopy [2] and for lower incident energy values for symmetric and asymmetric situations [3]. This has permitted the verification of the different theoretical models proposed [4], especially in the description of the correlated electronic continuum [5].

In spite of the fact that it is easier to obtain diatomic targets, which exist naturally in gaseous form, $(e,2e)$ experiments are less frequent on diatomic systems [6,7] than on atoms. The basic reason for this is that very-high-energy resolution is necessary to distinguish between the levels of the residual ion (Fig. 2). From the theoretical point of view one has to underline that the basic two-center Coulomb wave has not yet found an appropriate expression, although the exact solutions of the corresponding two-center Schrödinger equation that is separable in spheroidal coordinates have been largely studied for the positive energy domain [8–10].

The aim of the present work is to realize a comparative study of the $(e,2e)$ ionization of three isotopes H_2, D_2, or T_2 to show for further experimental applications the similar and particular aspects of their multiply differential cross sections in the case of high incident electron energy values (4 keV). Assuming that vertical transitions (Fig. 2) between the lowest vibrational level of the fundamental $^1\Sigma_g$ electronic state of H_2, D_2, or T_2 and all the vibrational levels of the $^2\Sigma_g$ electronic state of H_2^+, D_2^+, or T_2^+, respectively, are preponderant, one can express the multiply differential cross section of an $(e,2e)$ reaction as the product of an electronic transition matrix element and the probability density of having the diatomic system at a given internuclear distance. This appears to be a good compromise that makes the introduction of the vibrational effects possible in an adiabatic regime.

THEORY

The system of axis used for our study is defined in Fig. 1(a). The origin coincides with the center of the diatomic molecule and the z axis is taken parallel to the direction of the impinging electron. The vectors $\vec{\rho}$, $\vec{R}$, $\vec{r}_1$, and $\vec{r}_2$ shown

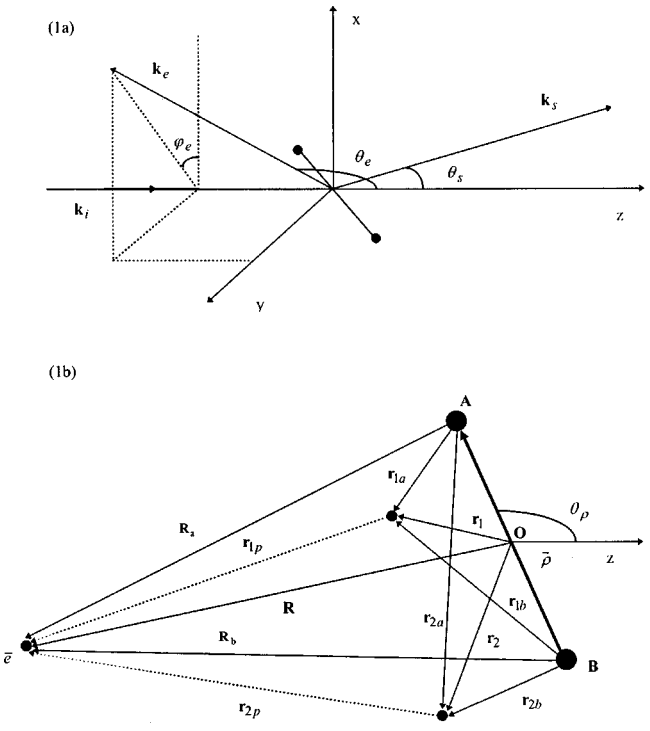

FIG. 1. (a) The reference frame with the different wave vectors $\vec{k}_i$, $\vec{k}_s$, and $\vec{k}_e$ representing the incident, scattered, and ejected electrons, respectively. θ_s, θ_e denote the scattering and the ejection polar angles, respectively, and φ_e the azimuthal ejection angle. (b) The different position vectors of the incident and the bound electrons with respect to the two nuclei.

on Fig. 1(b) define, respectively, the positions of the nuclei, the incident electron, and the two target electrons. We admit that the ionization process of a diatomic system by fast electrons is purely an electronic transition for a given $\vec{\rho}$ and write the sevenfold cross section for an $(e,2e)$ experiment as follows:

$$\sigma^{(7)}_{n_f,n_i}=\frac{d^7\sigma}{d\Omega_\rho d\Omega_e d\Omega_s d(k_s^2/2)}=\frac{(2\pi)^4 k_e k_s}{k_i}\int_0^\infty \rho^2 d\rho |\Xi_{n_f}(\rho)|^2 |\Theta_{n_i}(\rho)|^2 |t^e_{fi}(\vec{\rho})|^2, \tag{1}$$

where Ω_ρ, Ω_e, and Ω_s represent, respectively, the solid angles corresponding to $\vec{\rho}$, to the ejected electron, and to the scattered electron; k_i, k_s, k_e are the moduli of the wave vectors [Fig. 1(a)]. $|\Xi_{n_f}(\rho)|^2$ and $|\Theta_{n_i}(\rho)|^2$ represent the probability densities of having the nuclei at a given relative distance ρ in the final vibrational n_f state and initial vibrational n_i state. Finally, $t^e_{fi}(\vec{\rho})$ represents the habitual electronic transition matrix element given by the first-order term of the Born approximation:

$$t^e_{fi}(\vec{\rho})=\langle \Psi_f^-(\vec{\rho},\vec{R},\vec{r}_1,\vec{r}_2)|V|\Psi_i(\vec{\rho},\vec{R},\vec{r}_1,\vec{r}_2)\rangle. \tag{2}$$

Here the integration runs over $\vec{R}$, $\vec{r}_1$, and $\vec{r}_2$. Ψ_i and Ψ_f^- are the wave functions that correspond, respectively, to the initial and final electronic states of the system for a given value of $\vec{\rho}$. V represents the interaction between the incident electron and the target [Fig. 1(b)]:

$$V=-\frac{Z}{R_a}-\frac{Z}{R_b}+\frac{1}{r_{1p}}+\frac{1}{r_{2p}}. \tag{3}$$

We designate the ionization potential for a given transition by $I^+_{n_f,n_i}$ which satisfies the energy conservation:

$$E_i=I^+_{n_f,n_i}+E_s+E_e, \tag{4}$$

where E_i, E_s, and E_e represent, respectively, the energy values of the incident, scattered, and ejected electrons. Now, if in a given $(e,2e)$ process the orientation of the molecule is not observed, one must average on all possible molecular orientations. Equation (1) then gives the fivefold differential cross section for a given transition:

$$\sigma^{(5)}_{n_f,n_i}=\frac{d^5\sigma}{d\Omega_e d\Omega_s d(k_s^2/2)}=\frac{1}{4\pi}\int d\Omega_\rho \sigma^{(7)}_{n_f,n_i}. \tag{5}$$

The electronic transition matrix element of an $(e,2e)$ reaction for two electron targets is treated by Schulz [11]. This results in three types of terms corresponding to the direct term, where the scattered electron has the same label as the incident one, the exchange term, where the ejected electron has the same label as the incident electron, and finally the ''capture'' term, where the index of incident electron is attributed to the bound electron of the residual ion.

In the cinematically asymmetric situations ($E_s \gg E_e$) studied in this paper, the exchange and the capture terms as defined above are negligible with respect to the direct term, which we will write in the following form:

$$t^e_{fi}(\vec{\rho})=\left\langle \frac{e^{i\vec{k}_s\cdot\vec{R}}}{(2\pi)^{3/2}} G(\vec{k}_e,\vec{r}_1)\Phi_{1_s\sigma_g}(r_2,\rho)\right| \times V\left|\frac{e^{i\vec{k}_i\cdot\vec{R}}}{(2\pi)^{3/2}}\Phi_{1\Sigma_g^+}(r_1,r_2,\rho)\right\rangle. \tag{6}$$

Here the fast incident and the scattered electron are described by plane-wave functions. The diatomic target molecule in its ground $^1\Sigma_g^+$ state is given by a Heitler-London [12] type wave function:

$$\Phi_{1\Sigma_g^+}(\rho,\vec{r}_1,\vec{r}_2)=N(\rho)\{e^{-\alpha r_{1a}}e^{-\alpha r_{2b}}+e^{-\alpha r_{1b}}e^{-\alpha r_{2a}}\}, \tag{7}$$

obtained by applying a variational method. In the final state, we describe the ejected electron as in [13] by a Coulomb wave function of the form

$$C(\vec{k},\vec{r},\gamma)=\frac{e^{(-\pi\gamma/2)}}{(2\pi)^{3/2}}\Gamma(1-i\gamma)e^{i\vec{k}\cdot\vec{r}} \times {}_1F_1(i\gamma,1;-i(k_e r+\vec{k}_e\cdot\vec{r})) \tag{8}$$

in such a way that

$$G(\vec{k}_e,\vec{r}_1)=C(\vec{k}_e,\vec{r}_{1j},\gamma) \tag{9}$$

with $r_{1j}=r_{1a}$ or r_{1b} [Fig. 1(b)] depending on the initial center of the ejected electron [13,14] and $\gamma=-\alpha/k_e$. This choice of the initial-state parameter α in the final state is justified by the fact that α represents approximately the charge of the two screened nuclei in the asymptotic limit. More, it allows us to avoid the calculation of very cumbersome terms in Eq. (6), which, as we verified separately, are always negligible for all values of γ. Replacing these expressions in Eq. (6) we obtain

$$t^e_{fi}(\vec{\rho})=\frac{N(\rho)}{(2\pi)^3}\{p_a(\vec{\rho})+p_b(\vec{\rho})\} \tag{10}$$

with

$$p_a(\vec{\rho})=\langle e^{i\vec{k}\cdot\vec{R}}C(\vec{k}_e,\vec{r}_{1a},\gamma)\Phi_{1_s\sigma_g}(\vec{r}_2,\rho)|V|e^{-\alpha r_{1a}}e^{-\alpha r_{2b}}\rangle, \tag{11}$$

where $\vec{k}=\vec{k}_i-\vec{k}_s$ represents the momentum transfer.

The bound electron of the residual ion H_2^+ is also described by linear combination of atomic orbitals [15]:

$$\Phi_{1_s\sigma_g}(\vec{r},\rho)=M(\rho)\{e^{-\beta r_a}+e^{-\beta r_b}\}. \tag{12}$$

The expressions of $p_a(\vec{\rho})$ and $p_b(\vec{\rho})$ obtained in the Appendix permit us to write the electronic transition matrix element in the form

$$t^e_{fi}(\vec{\rho})=\frac{2N(\rho)M(\rho)}{(\pi)^{5/2}k^2}\cos\left(\vec{k}\cdot\frac{\vec{\rho}}{2}\right)\omega(\vec{k}_e,\vec{k}-\vec{k}_e,\gamma,\alpha) \times\{J(\beta,\alpha)+J(0,\beta+\alpha)\} \tag{13}$$

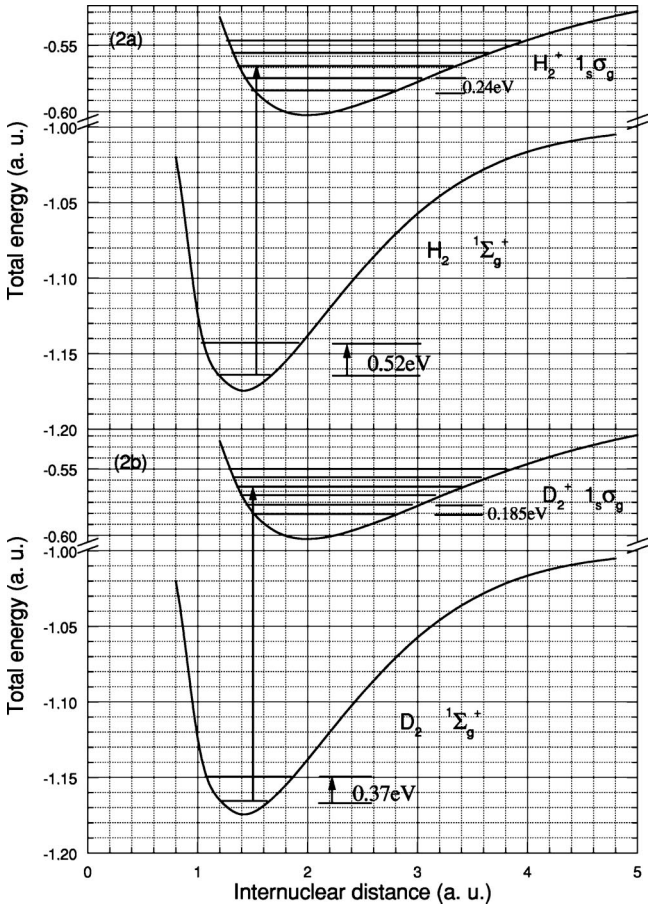

FIG. 2. The initial and final potential wells, with the different vibrational levels corresponding to H_2 and D_2 and the corresponding residual ions H_2^+ and D_2^+.

with $J(\nu,\mu)=\int d\vec{r}\, e^{-(\nu r_a+\mu r_b)}$ and

$$\omega(\vec{k},\vec{q},\gamma,\alpha)=\int d\vec{r}\, e^{-i\vec{q}\cdot\vec{r}} e^{-\alpha r}\, {}_1F_1(-i\gamma,1;i(kr+\vec{k}\cdot\vec{r})),$$

which is a simplified Nordsieck-type integral [16] having a simple analytical expression.

The modifications, that the application of more elaborate electronic initial- [17] and final- [18] state wave functions can bring in the determination of the electronic transition matrix element [Eq. (6)], will be studied in a planned following paper. This can be done by long and time-consuming procedures, in contrast to the present work. In the meantime, we can already say that, as the modifications concern only the electronic part, which is common to the three isotopes, the general observations of the present work will not be affected.

RESULTS

As we mentioned above, we consider the ionization of H_2, D_2, and T_2 by fast electron impact as a vertical transition from the lowest vibrational level of the fundamental $^1\Sigma_g$ state potential well of each target to a given level of the fundamental $^2\Sigma_g$ state of H_2^+, D_2^+, or T_2^+, as shown in Fig. 2. One of the principal aims of the present work is to study the influence of introducing the mass of the nuclei in the ionization of H_2 and its isotopes. Recently, there has been a new interest concerning this aspect in photodouble ionization of H_2 and D_2 [19,20]. Our procedure, which factors out the nuclear probability density from the electronic transition matrix element [Eq. (5)], is very well adapted to show the differences between these three species, which reside mainly in their initial and final vibrational state probability densities given, respectively, by $|\Theta_{n_i}(\rho)|^2$ and $|\Xi_{n_f}(\rho)|^2$.

TABLE I. The ionization energy values from the fundamental state of H_2, D_2, and T_2 to the corresponding vibrational levels of H_2^+, D_2^+ and T_2^+.

$n_i=0\rightarrow n_f$	Ionization energies l_{nf} (a.u.)		
	H_2	D_2	T_2
0	0.567 149	0.568 513	0.569 116
1	0.577 137	0.575 701	0.575 034
2	0.586 544	0.582 593	0.580 753
3	0.595 391	0.589 198	0.586 279
4	0.603 692	0.595 522	0.591 614
5	0.611 463	0.601 571	0.596 762
6	0.618 712	0.607 351	0.601 727
7	0.625 449	0.612 865	0.606 511
8	0.631 676	0.618 118	0.611 117
9	0.637 396	0.623 113	0.615 547
10	0.642 607	0.627 851	0.619 804
11	0.647 304	0.632 335	0.623 888
12	0.651 477	0.636 565	0.627 8
13	0.655 113	0.640 542	0.631 543
14	0.658 195	0.644 263	0.635 116
15	0.660 697	0.647 826	0.638 519
16	0.662 592	0.650 935	0.641 753
17	0.663 845	0.653 878	0.644 817
18	0.664 438	0.656 554	0.647 71
19		0.658 956	0.650 43
20		0.661 077	0.652 977
21		0.662 91	0.655 348
22		0.664 442	0.657 539
23		0.665 664	0.659 609
24		0.666 562	0.661 373
25		0.667 128	0.663 006
26		0.667 377	0.664 444
27			0.665 681
28			0.666 71
29			0.667 525
30			0.668 12
31			0.668 493
32			0.668 661

We have obtained $|\Theta_{n_i}(\rho)|^2$ by solving numerically, for each isotope with the appropriate reduced masses μ, the following radial equation:

$$\frac{d}{\rho^2 d\rho}\left[\rho^2\frac{d\Theta_n(\rho)}{d\rho}\right]+2\mu[\varepsilon_n-U_{1_{\Sigma_g^+}}(\rho)]\Theta_n(\rho)=0, \tag{14}$$

where the potential $U_{1_{\Sigma_g^+}}(\rho)$, given in [17], is obtained by solving the electronic equation of H_2. On the other hand,

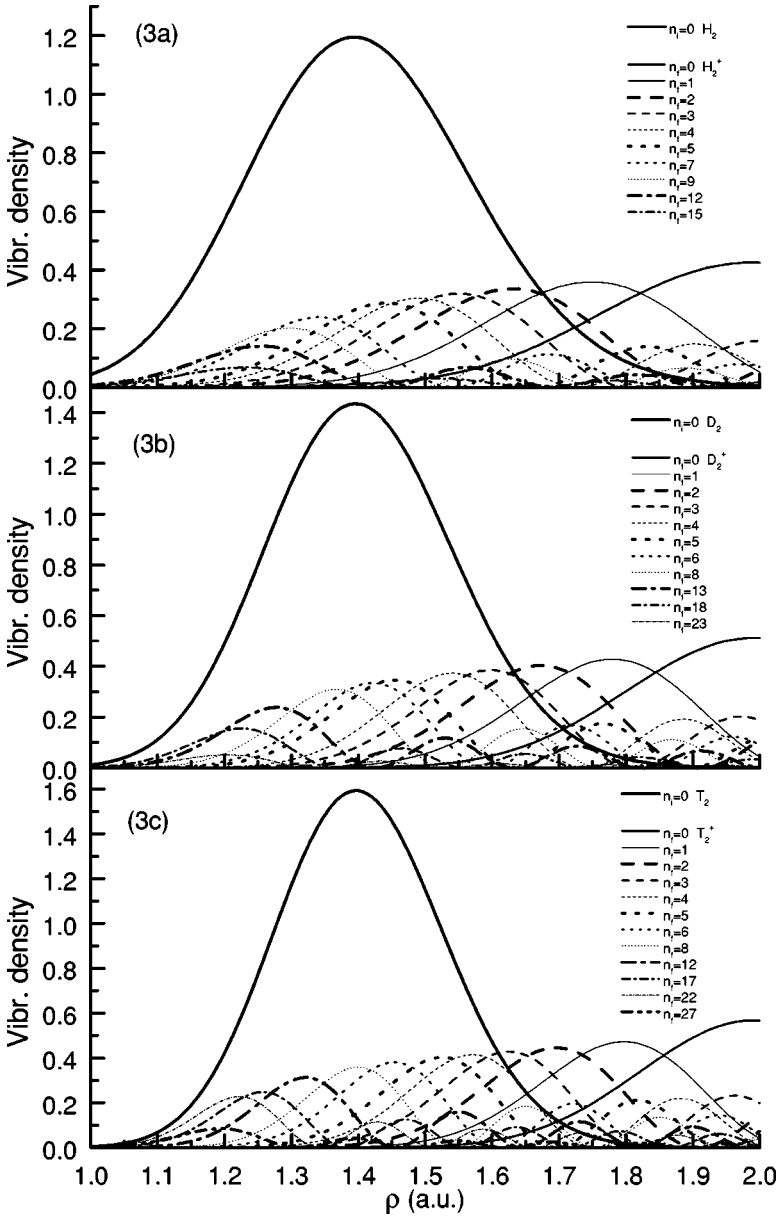

FIG. 3. The variation of the fundamental $|\Theta_0(\rho)|^2$ vibrational probability density in large full lines and those of the final-state ions $|\Xi_{n'}(\rho)|^2$ in terms of the internuclear distance ρ. (a) corresponds to H_2 and H_2^+, (b) to D_2 and D_2^+, (c) to T_2 and T_2^+.

$|\Xi_{n_f}(\rho)|^2$ are obtained for H_2^+, D_2^+, and T_2^+ by solving the same equation (14) with the potential $U_{2\Sigma_g}(\rho)$ corresponding to the adiabatic solution of the electronic equation H_2^+ given in [21]. We have verified our results by comparing our vibrational energy values ε_n to those given in [17] and [21].

In Table I, we present the ionization potentials I_{n_f} corresponding to the energy difference between $n_i=0$ of a target and $n_f=0,1,2,3,\ldots,N_f$ of the corresponding ion. N_f corresponds to the highest level that reaches the dissociation limit.

We also present in Figs. 3(a)–3(c) the variation of the probability densities in terms of the internuclear distance ρ of the three species as indicated. On each figure the large curves with full lines centred on $\rho=1.4$ a.u. correspond to that of the fundamental state of the target; the others correspond to the different levels of the respective ions designated by n_f. It is interesting to observe that $|\Theta_0(\rho)|^2$ for the three isotopes vanishes outside the domain $1\leqslant\rho\leqslant 2$ a.u., and that $|\Xi_{n_f}(\rho)|^2$ for $n_f=0,1,2$ are relatively small in this domain. This means that most of the (ionization) events will take place in this region, and that the states corresponding to $n_f=0,1,2$ will have a very small participation on the total fivefold differential cross sections (5DCS) as we will observe below.

Actual $(e,2e)$ setups do not have the necessary energy resolution to distinguish between two neighboring levels. The experimental setup of Chérid *et al.* [7], for instance, has an energy resolution of about 3 eV for an incident energy of 4000 eV and that of Jung *et al.* [22] about 0.5 eV for an incident energy of 250 eV. This means that the experimental value of 5DCS will correspond to the sum of the theoretical 5DCS corresponding to the levels found in the given energy domain such that

$$\sigma^{(5)}=\sum_{n_f=n_0}^{n_0+M_f}\sigma_{n_f}^{(5)}, \tag{15}$$

where $\sigma_{n_f}^{(5)}$ correspond to $\sigma_{n_f,0}^{(5)}$ given by Eq. (5), and where M_f represents the number of the vibrational levels of the

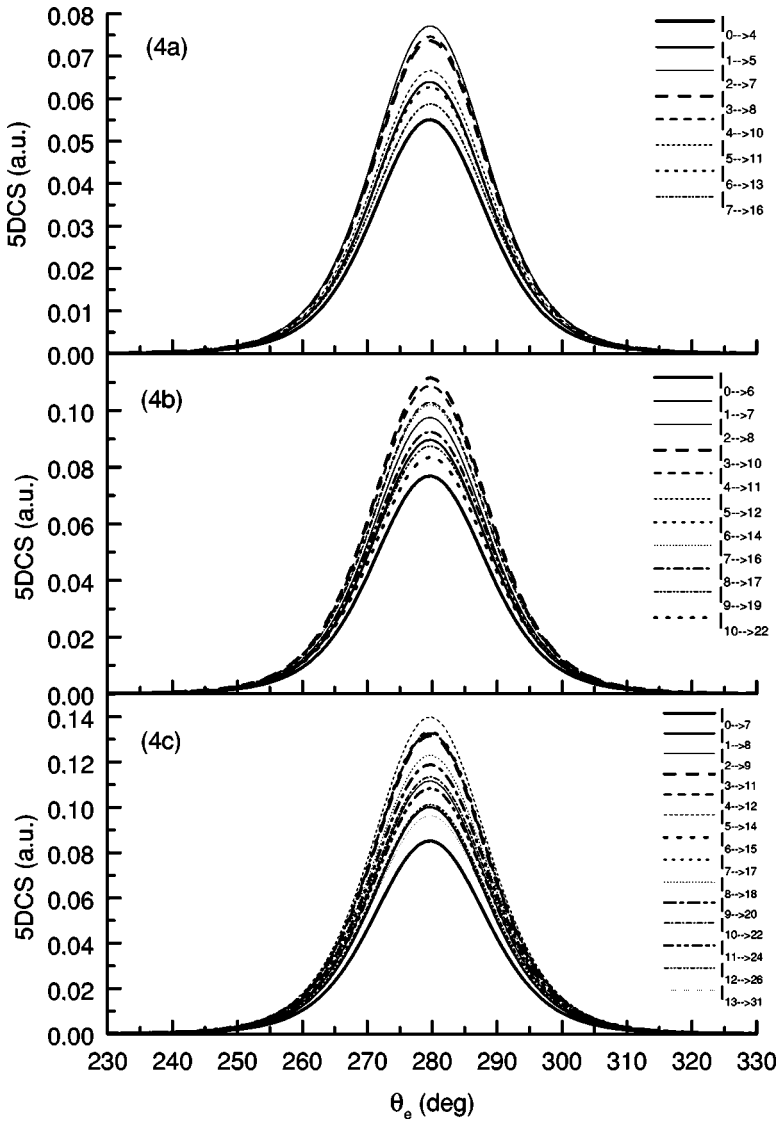

FIG. 4. The variation of the fivefold differential cross section (5DCS) of the $(e,2e)$ ionization of H_2, D_2, and T_2 in terms of the ejection angle θ_e for an energy resolution of 1 eV. The incident and the ejected electron energies are 4168 eV and 100 eV, respectively; the scattering angle $\theta_s = 8.9°$. The different curves correspond to the transition designated. (a) corresponds to the transitions from H_2 to H_2^+, (b) to those of D_2 to D_2^+, and (c) to those of T_2 to T_2^+.

residual ion involved for a given energy resolution, n_0 being the label of the first level involved.

Choosing an energy resolution around 1 eV, we present in Figs. 4(a)–4(c) the variation of the 5DCS given in Eq. (15) for H_2, D_2, and T_2, respectively, for an asymmetric situation with an incident electron energy value of 4168 eV (setup of Chérid *et al.* [7]), and an ejected electron energy value of 100 eV, for a scattering angle $\theta_s = 8.9°$ corresponding to the favorable situation, where $|\vec{k}| = |\vec{k}_e|$, which results, for the particular value of the ejection angle $\theta_e = 280°$, in a recoil momentum $\vec{k}_{\text{recoil}} = \vec{k} - \vec{k}_e$ equal to zero (Bethe ridge). This, as we observe on these figures, is confirmed for all the curves corresponding to different n_0 that have their maximum at this particular angle. It is also observed that, in the case of molecular hydrogen, the 5DCS involving I_2^+ to I_7^+ is relatively more important than the others. In the case of D_2 we must underline the fact that, for the same experimental resolution of 1 eV, we have one or more extra levels to consider as the levels are nearer to each other (Table I) and the predominant 5DCS corresponds to that involving the transitions I_3^+ to I_{10}^+. The same observation can be done in the case of T_2 for which the levels are still more concentrated. Here the predominant 5DCS correspond to those going from I_5^+ to I_{14}^+ involving nine levels. These observations can be explained by the positions of the maxima of the curves corresponding to the different vibrational densities of the ions given in Figs. 3(a)–3(c). From this point of view one can say that an $(e,2e)$ experiment on a diatomic system can eventually probe the densities of the vibrational levels of the final-state ions.

For experiments with lower-energy resolution ($\approx$3 eV) comparable to the dissociation energy of the residual ion, we consider all the levels present in the corresponding potential well given in Table I. Figure 5 shows the variation of the total 5DCS for the three molecules in terms of the ejection angle. In contrast to the higher-energy resolution case [Figs. 4(a)–4(c)] where the differences between the 5DCS of the three molecules are around 0.04 a.u., here they are of the order of 0.1 a.u. This confirms what has been lately observed [19] in the measurement of the multiply differential cross section of the photodouble ionization of H_2 and D_2 where a significant difference has been measured between the cross sections of the two molecules. Later [20], this difference has been observed to diminish for higher-energy resolutions exactly as in our case.

It has been sometimes considered [7] that, as the equilibrium internuclear distance of the fundamental level of H_2 is

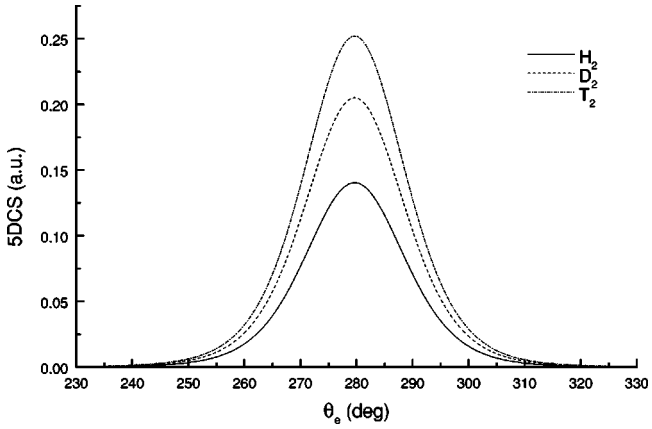

FIG. 5. The variation of the 5DCS of the $(e,2e)$ ionization of H_2 (full curve), D_2 (dashed curve), and T_2 (dash-dot curve) in terms of the ejection angle θ_e for an energy resolution of 3 eV. The incident and the ejected electron energies are 4168 eV and 100 eV, respectively, the scattering angle $\theta_s = 8.9°$.

at about $\rho = 1.4$ a.u., most of the ionization events should occur at this distance. In Fig. 6, where the variation of the 5DCS of the three systems is given in terms of the internuclear distance ρ for fixed values of $\theta_s = 8.9°$ and $\theta_e = 280°$ in two resolutions (1 and 3 eV), one can see that this approximation is not always true especially in the cases of higher resolution (1 eV) where the curves are not centered on the equilibrium position.

Figure 7 shows, for a low resolution (3 eV), the variation of the total 5DCS of H_2 in terms of the ejection and scattering angles in the above asymmetric case (4168 eV, 100 eV). For scattering angles higher than 15°, the 5DCS is negligible as expected. The maximum around $\theta_s = 8.9°$ represents the Bethe ridge as mentioned above. It is also observed that, for small scattering angles ($\theta_s < 2°$), the ejected electron has the tendency to emerge in the forward direction ($\theta_e = 350°$) for this high incident electron energy value. This can be explained by the fact that, at small scattering angles, the momentum transfer is very small and is oriented in the forward direction. Now, the recoil momentum ($\vec{k}_{\text{recoil}} = \vec{k} - \vec{k}_e$) will be optimal in two situations, when the ejection direction is parallel to it or antiparallel to the momentum transfer $\vec{k}$ and thus to $\vec{k}_{\text{recoil}}$. These two favorable situations are represented by the two picks that we observe at $\theta_e = 170°$ and 350° as expected.

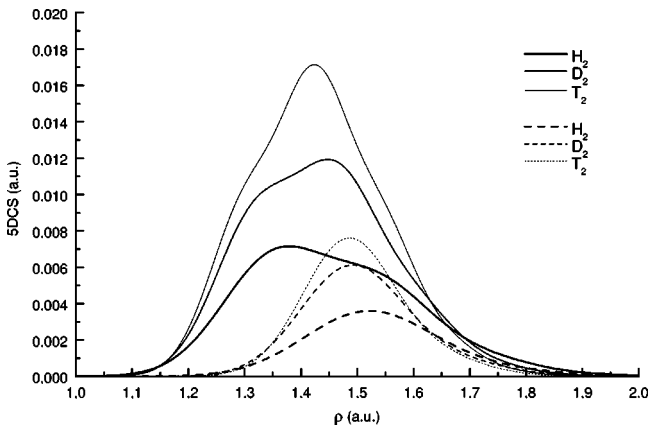

FIG. 6. The variation of the 5DCS of the $(e,2e)$ ionization of H_2, D_2, and T_2 in terms of the internuclear distance ρ for two energy resolutions 1 eV (dashed curves) and 3 eV (full curves). For the same energy conditions as in Fig. 4.

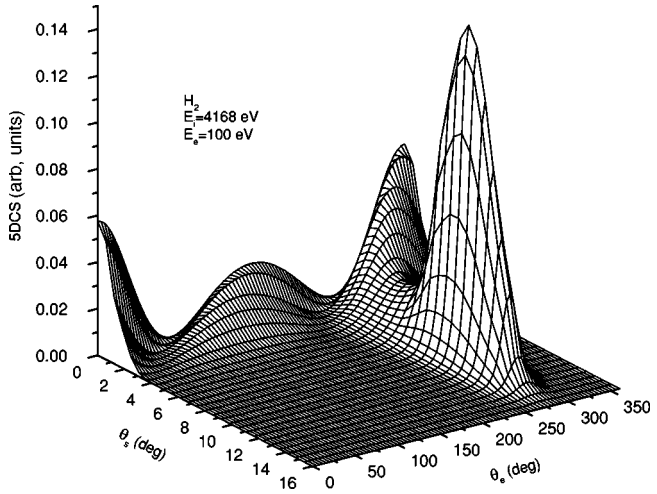

FIG. 7. The variation of the 5DCS of the $(e,2e)$ ionization of H_2 in terms of the scattering and the ejection angles for the same energy conditions as in Fig. 4.

CONCLUSION

We have developed a procedure for the determination of the multiply differential cross section of the $(e,2e)$ ionization of molecular hydrogen and its two isotopes considered as a vertical transition, which permits the introduction of vibrational probability densities of the initial and the final states. As the three molecules present the same adiabatic electronic structure, it is shown that the 5DCS depends strongly on the energy resolution of the experimental setup. The experimental verification of these results, as was done in the case of photodouble ionization, will open the way for further measurements on heavier diatomic targets such as nitrogen or sodium, whose vibrational levels in the initial and final state are much closer having consequently temperature-dependent population densities, in contrast to H_2, D_2, and T_2, which are considered to be initially in their fundamental state as very high temperatures (thousands of degrees) are necessary to have them vibrationally excited.

APPENDIX

To *determine*

$$p_a = \left\langle e^{i\vec{k}\cdot\vec{R}} C(\vec{k}_e, \vec{r}_{1a}, \alpha) \Phi_{1_s\sigma_g}(r_2, \rho) \left| \frac{1}{r_{1p}} \right| \{ e^{-\alpha r_{1a}} e^{-\alpha r_{2b}} \} \right\rangle,$$

we write

$$p_a = \left\langle e^{i\vec{k}\cdot\vec{R}} C(\vec{k}_e, \vec{r}_{1a}, \alpha) \left| \frac{1}{r_{1p}} \right| e^{-\alpha r_{1a}} \right\rangle \langle \Phi_{1_s\sigma_g}(r_2, \rho) | e^{-\alpha r_{2b}} \rangle. \tag{A1}$$

Using the relations $r_{1p} = |\vec{R}_a - \vec{r}_{1a}|$, $\vec{R} = \vec{R}_a + \vec{\rho}/2$ [Fig. 1(b)] we obtain

$$p_a = e^{i\vec{k}\cdot\vec{\rho}/2}\langle \Phi_{1_s\sigma_g}(r_2,\rho)|e^{-\alpha r_{2b}}\rangle \times \int C(\vec{k}_e,\vec{r}_{1a},\alpha)e^{-\alpha r_{1a}}d\vec{r}_{1a}\int \frac{e^{i\vec{k}\cdot\vec{R}_a}}{|\vec{R}_a-\vec{r}_{1a}|}d\vec{R}_a \tag{A2}$$

as

$$\int d\vec{R}\frac{e^{i\vec{k}\cdot\vec{R}}}{|\vec{R}-\vec{r}|} = \frac{4\pi}{k^2}e^{i\vec{k}\cdot\vec{r}},$$

$$p_a = e^{i\vec{k}\cdot\vec{\rho}/2}\sqrt{2/\pi}\,\frac{M(\rho)}{k^2}\,\omega(\vec{k}_e,\vec{k}-\vec{k}_e,\alpha) \times\{J(\beta,\alpha)+J(0,\beta+\alpha)\} \tag{A3}$$

with $J(\nu,\mu)=\int d\vec{r}\, e^{-(\nu r_a+\mu r_b)}$ and

$$\omega(\vec{k},\vec{q},\lambda) = \int d\vec{r}\, e^{-i\vec{q}\cdot r-\lambda r}\,{}_1F_1(-i\alpha_e,1;i(kr+\vec{k}\cdot r)),$$

which represents a particular case of the Nordsieck integral [16] that can be given in simple analytical expressions.

In a similar way we can obtain

$$p_b = e^{-i\vec{k}\cdot\vec{\rho}/2}\sqrt{2/\pi}\,\frac{M(\rho)}{k^2}\,\omega(\vec{k}_e,\vec{k}-\vec{k}_e,\alpha) \times\{J(\beta,\alpha)+J(0,\beta+\alpha)\} = e^{-i\vec{k}\cdot\rho}p_a\,. \tag{A4}$$

[1] C. Champion, A. L'Hoir, M. F. Politis, A. Chetioui, B. Fayard, and A. Touati, in *Proceedings of the Fourth International Conference on Swift Heavy Ions in Matter*, Berlin, 1998, edited by S. Klaumünzer and N. Stolterfoht (North-Holland, Elsevier, Amsterdam, 1998), pp. 533–540.

[2] E. Weigold and I. E. Mc Carthy, Phys. Rep., Phys. Lett. **27**C, 275 (1976).

[3] H. Ehrhardt, K. Jung, G. Knoth, and P. Schlemmer, Z. Phys. D **1**, 3 (1986).

[4] C. T. Whelan *et al.*, (*e*,2*e*) & *Related Processes* (Kluwer Academic, Boston, 1993), pp. 33–74.

[5] M. Brauner, J. S. Briggs, and H. Klar, J. Phys. B **22**, 2265 (1989).

[6] R. W. Zurales and R. R. Lucchese, Phys. Rev. A **35**, 2852 (1987).

[7] M. Chérid, A. Lahmam-Bennani, R. W. Zurales, R. R. Lucchese, A. Duguet, M. C. Dal Capello, and C. Dal Cappello, J. Phys. B **22**, 3483 (1989).

[8] P. J. W. Greenland and W. Greiner, Theor. Chim. Acta **42**, 273 (1976).

[9] L. I. Ponomarev and L. N. Somov, J. Comput. Phys. **20**, 183 (1976).

[10] Y. S. Tergiman, Phys. Rev. A **48**, 88 (1993).

[11] M. Schulz, J. Phys. B **6**, 2580 (1973).

[12] J. C. Slater, *Quantum Theory of Molecules and Solids* (McGraw-Hill, New York, 1963), Vol. 1, pp. 22–53.

[13] J. Hanssen, B. Joulakian, R. Rivarola, and R. J. Allan, Phys. Scr. **53**, 41 (1996).

[14] Y. D. Wang, J. H. McGuire, and R. D. Rivarola, Phys. Rev. A **40**, 3673 (1989).

[15] C. A. Coulson, Trans. Faraday Soc. **33**, 1479 (1937).

[16] A. Nordsieck, Phys. Rev. **93**, 785 (1954).

[17] W. Kolos, K. Szalewicz, and H. J. Monkhorst, J. Chem. Phys. **84**, 3278 (1986).

[18] B. Joulakian, J. Hanssen, R. D. Rivarola, and A. Motassim, Phys. Rev. A **54**, 1473 (1996).

[19] J. P. Wightman, S. Cvejanovic', and T. J. Reddish, J. Phys. B **31**, 1753 (1998).

[20] J. P. N. Scherer, H. Lörch, and V. Schmidt, J. Phys. B **31**, L817 (1998).

[21] D. M. Bishop and R. W. Wetmore, Mol. Phys. **26**, 140 (1973).

[22] K. Jung, E. Schubert, D. A. L. Paul, and H. Ehrhardt, J. Phys. B **8**, 1330 (1975).